Limnol. Oceanogr., 45(6), 2000, 1401–1408

Expansion of a moraine-dammed glacial lake, Tsho Rolpa, in Rolwaling Himal, Nepal Himalaya

Akiko Sakai[1]
Institute for Hydrospheric–Atmospheric Sciences, Nagoya University, Nagoya 464-8601, Japan

Kazuhisa Chikita
Division of Earth and Planetary Sciences, Graduate School of Science, Hokkaido University, Sapporo 060-0810, Japan

Tomomi Yamada
Institute of Low Temperature Science, Hokkaido University, Sapporo 060-0819, Japan

Abstract

Across the surface of debris-covered glaciers in the Nepal Himalayas there are many lakes on the order of 1 km in scale. Some of the lakes, dammed by the end/lateral moraine, have been expanded from ponds on the order of 100 m in length. Tsho Rolpa Glacier Lake in the headwater region of the Rolwaling Valley, Eastern Nepal, was probably a small pond in the early 1950s. The present expansion rate of the glacial lake is unknown. From our investigation of the hydrological and meteorological conditions in 1993–1994, the calculated heat balance in the lake showed a deepening rate of about 1.2 m yr^{-1} all through the year. This is comparable to the mean deepening rate of the bottom basin since 1952. The vertical expansion thus is still continuing. Annual volume expansion including the calving ice (horizontal expansion) volume was 3% of the present total volume of the lake.

There are many glacial lakes that were glacier-dammed or moraine-dammed in Iceland, Norway, Alaska, Peru, New Zealand, and several other countries (Thorarinsson 1939, 1957; Liestøl 1956; Post and Mayo 1971; Lliboutry 1977; Lliboutry et al. 1977*a,b*; Kirkbride 1993). Such glacial lakes sometimes produced outburst floods, a phenomenon called glacial lake outburst flood (GLOF).

In the Himalayas, large valley glaciers several kilometers long have a mostly debris-covered ablation area and occupy about 80% of the glacialized areas (Moribayashi 1974). Debris-covered glaciers have advanced to approximately 4,500 m above sea level in the Little Ice Age between the 16th and 19th centuries. At present some debris-covered glaciers are retreating due to the horizontal expansion of the glacial lakes that emerged during recent decades. The glacial lakes are surrounded and dammed by end moraines that formed in the Little Ice Age. Lake water overtopping a moraine carried sufficient energy to break easily through a moraine dam. This overtopping was caused by a large wave generated by a huge snow or ice mass falling down into the lake, such as in a snow or glacier avalanche down a steep slope beside the lake, or by advancing, sliding, and calving (ice wastage by shedding of large ice blocks from a glacier's edge into a body of water) of the mother glacier into the lake. Earthquakes may also act as external triggers contributing to lake outbursts.

Abundant meltwater from glaciers is the main water resource and provides abundant hydropower potential in Nepal. GLOF has occurred somewhere at least 13 times since the 1960s, and hydropower has been damaged. This phenomenon is, therefore, a serious natural disaster that can affect the development of water resources (Yamada 1993; Lanzhou Institute of Glaciology and Geocryology/Water and Energy Commission Secretariat/Nepal Electricity Authority [LIGG/WECS/NEA] 1988). There are still several glacial lakes upstream of hydropower facilities. A larger volume of stored water can cause a more serious disaster. Thus, it is important to know the expansion rate of a glacial lake in order to estimate future GLOF damage.

The horizontal enlargement of the glacial lakes has been determined from aerial photos and satellite images. Bathymetric maps of Tsho Rolpa Glacial Lake have been made to evaluate its volume (Yamada 1998), and the average deepening rates since the lake emerged (average depth at present/age of the glacial lake) were determined (Yamada 1995). Their present expansion rate, however, is yet to be measured because of accuracy problems. Therefore, the purpose of this study is to evaluate the present expansion rate of one glacial lake by the heat-balance method.

Background

The drainage area including the lake surface is 77.6 km^2 with 71.8% glacial coverage, 55.3% and 16.5% of which,

[1] Corresponding author (shakai@ihas.nagoya-u.ac.jp).

Acknowledgments

We thank T. Kadota for his generous support and advice in the field and two anonymous reviewers for their constructive comments on the manuscript. Our sincere thanks also to C. K. Sharma, H. M. Shrestha, and G. R. Bhatta, Executive Secretary, WECS. We are also indebted to K. P. Rizal, Officiating Executive Director, WECS, P. Mool, ICIMOD, Kiran Shankar Yogacharya, and Adarsha Pokhrel, Department of Hydrology and Meteorology (DHM), who officially supported and made arrangements for our research in the field. Financial support for our field work in Tsho Rolpa Glacier Lake was provided by JICA (Japan International Cooperation Agency) and a Grant-in-Aid for Scientific Research (chief: Yutaka Ageta, 1994, 06041051) from the Ministry of Education, Science, Sports, and Culture of Japan.

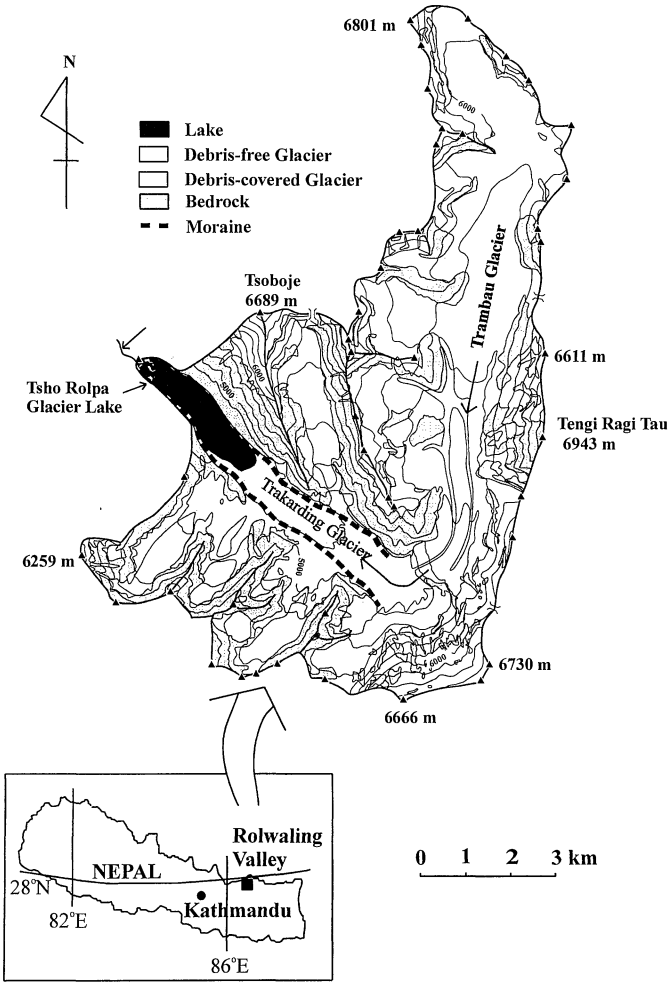

Fig. 1. Drainage basin of Tsho Rolpa Glacier Lake, Rolwaling Valley and its location in Nepal.

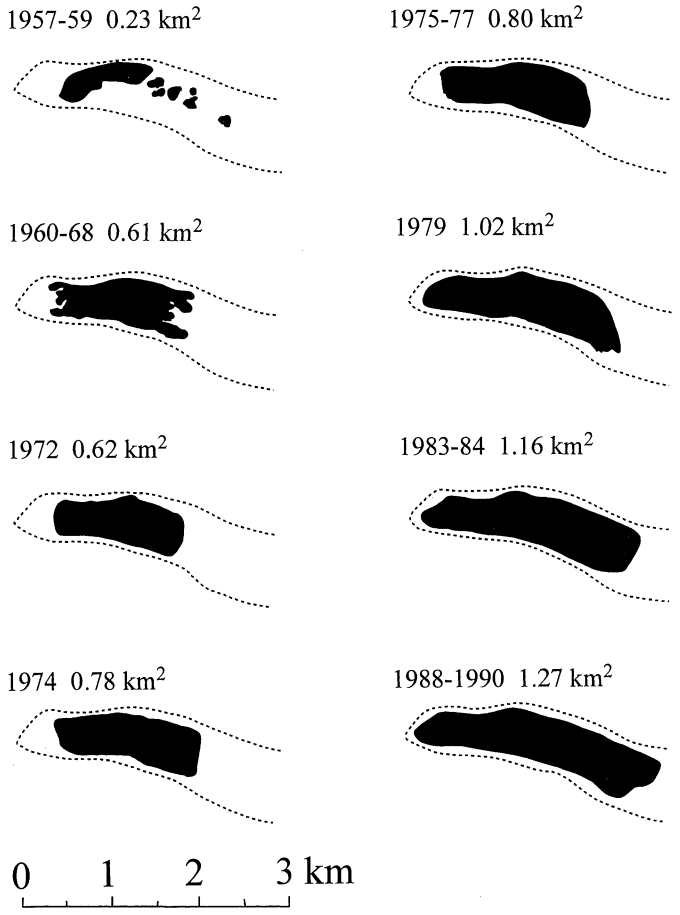

Fig. 2. Change in the surface area of Tsho Rolpa Lake from satellite images. Dashed-dotted lines indicate the moraine ridge (modified after Mool [1995]).

respectively, are occupied by a debris-free glacier (the Upper Trambau Glacier) and a debris-covered glacier (the Trakarding Glacier) (Yamada 1996) (Fig. 1; modified Schneider's topographic map; Schneider 1981). The lake surface area and the volume in 1994 were 1.39 km^2 and 76.6 $\times$ 10^6 m^3, respectively.

Figure 2 shows the expansion history of Tsho Rolpa Glacier Lake obtained by data from aerial photos, topographic maps, and satellite images (Earth Resources Technology Satellite [ERTS], Multispectral Scanner System [MSS], Marine Observation Satellite-1 [MOS 1], Multispectral Electronic Self-Scanning Radiometer [MESSR], and Landsat [MSS]) (Mool 1995). In 1958 the surface area was 0.23 km^2 according to a topographic survey by the Survey of India. Because the horizontal growth rate is almost constant, the lake probably appeared as a small pond around 1952.

Observation

Methods—Meteorological and hydrological observations were carried out in 1994 at Tsho Rolpa Lake (27°51′N, 86°29′E), Rolwaling Valley, Eastern Nepal (Fig. 1). Figure 3 shows the location of observation sites on the bathymetric map made in 1994 by Kadota (1994). The maximum depth is 131 m at site LD.

Site LM is a meteorological station on an islet. The four meteorological elements were measured hourly at 2.1 m above the ground from 8 June to 3 November 1994: Air temperature (T_a), wind velocity (Ws), relative humidity (Rh), and shortwave solar radiation ($I^{\downarrow}$). Their accuracies are 0.1°C, 0.1 m s^{-1}, 3%, 2 W m^{-2}, respectively. Surface water temperature of the lake (T_s) was also measured hourly at site LS by thermistor sensor (accuracy, ±0.4°C) fixed at a water depth of about 5 cm. Albedo was obtained at site LA by measuring both upward and downward shortwave radiation at intervals of 1 min in June 1994 on fine, cloudy, and rainy days.

Lake water drains from the outlet at site LO. Water level and temperature at the outlet were observed hourly. Their accuracies were ±3 cm and ±0.4°C, respectively. Water level was converted to water discharge with an exponential rating curve (r = 0.99) obtained by discharge measurements at various water levels at site LO. The accuracy of the discharge is ±0.3 m^3 s^{-1} (7%).

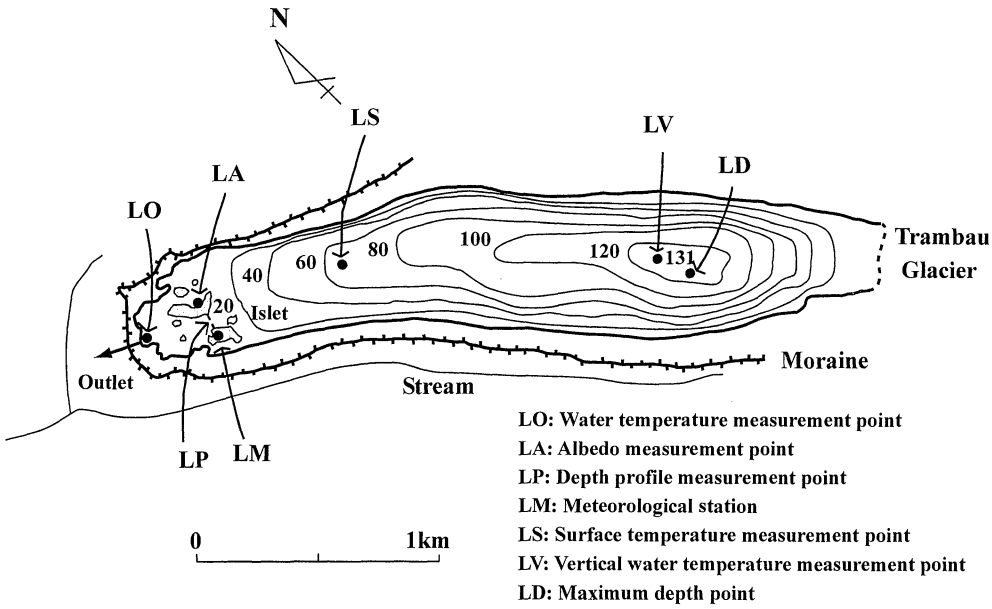

Fig. 3. Location of observation sites on the bathymetric map of Tsho Rolpa Lake. Numerical values indicate water depth in meters.

Vertical water temperature distributions were obtained by using a water temperature depth sensor at site LV near the deepest point on 8 June and 3 November 1994. These dates correspond to the beginning of the monsoon season and before ice-cover, respectively. Vertical water temperature profiles were also obtained on 7 November 1993 and 22 February 1994 corresponding to the ice-covered period. The accuracies of depth and water temperature are ±0.5 m and ±0.05°C, respectively.

Results—A time series of daily meteorological data from June to November are shown in Fig. 4a,b. The observed air temperature and wind speed during this period were on average 3.8°C and 2.3 m s^{-1}, respectively. In the Nepal Himalayas, the monsoon season usually begins in June and finishes in September. In the rainy season, the solar radiation was relatively low (about 199 W m^{-2} on average), and relative humidity was high with an average of 95%. The daily mean surface water temperature of the lake (T_s) and water temperature of the outflow (T_o) are shown in Fig. 4c (WECS 1994; Yamada 1995). T_o mean data were not obtained from 5 October to 3 November. The extrapolated T_o was evaluated from surface water temperature T_s that was always larger than T_o by 0.5°C (Fig. 4c). Water level was not obtained between 5 September and 15 November 1994. Discharge during the period of no water level data was estimated on the assumption that the water level decreased linearly over time in this period (−1.3 cm d^{-1}). The seasonal variation in daily discharge is shown in Fig. 4d, where the estimated data are shown by a dotted line. The discharge increased greatly in early June when the glacier melt started and peaked in early July; thereafter, it decreased gradually until early November. Such an annual variation in discharge is usual in the Nepal Himalayas (Sakai et al. 1997).

Seasonal data on vertical water temperature at site LV are shown in Fig. 5. Seasonal temperature fluctuation ranging from 0 to 6°C can be seen in the surface layer, for depths <50 m. Below this depth, the temperature remained roughly constant at around 2.7°C, in spite of the maximum density of pure water at 4°C. This is due to high suspended sediment concentrations in the lake that reached >100 mg L^{-1} at the surface and >300 mg L^{-1} at the bottom. The bulk water density depends on suspended sediment concentration (SSC) rather than water temperature. Suspended sediment is mainly transported into the lake by cold and highly turbid en-glacial meltwater (Yamada 1996). Figure 6 shows vertical profiles of water temperature, T_w, suspended sediment concentration, C, and water density in situ, σ_w, at site LD on 9 June 1994. σ_w is here defined by $\sigma_w = (\rho_{PTC} - 1{,}000) \times 10$, where ρ_{PTC} is bulk water density (kg m^{-3}) at C mg L^{-1}, T_w °C, and, given by $\rho_{PTC} = (1 - C \times 10^{-3}/\rho_s)\rho_C + C \times 10^{-3}$ (ρ_s, suspended sediment density, 2,730 kg m^{-3} for Tsho Rolpa Lake; ρ_C, clear water density at T_w °C and P Pa). The water compressibility was here given as 0.00045 per equivalent pressure ($P \cong 980{,}000$ Pa) at 100 m depth. Vertical distributions of water temperature, suspended sediment, and water density in situ, σ_w, showed a similar tendency throughout the year. Tsho Rolpa thus exhibits stable density stratification throughout the year, because SSC increased consistently with depth.

Although water temperatures in the deep layers are almost uniform over all the seasons, there exist some layers in which water temperatures were slightly different (about 0.5°C). Such a small difference may be due to the interflow of glacier-melt water that contained considerable suspended sediment (Chikita et al. 1999).

A temporal variation in the partial bottom topography was obtained between two islets uplake of the end moraine at site LP (see Fig. 3 for location). The deepening amount was

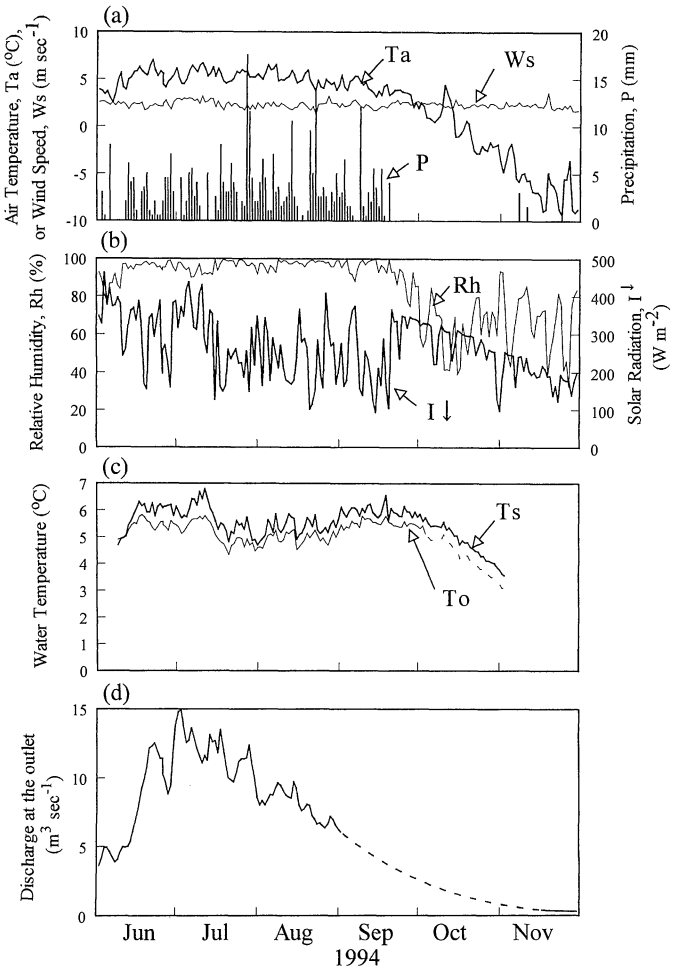

Fig. 4. Temporal variations in daily average data (a) air temperature, T_a, and wind speed, *Ws*; (b) relative humidity, *Rh,* and solar radiation $I^{\downarrow}$; (c) water temperatures, T_s at the lake surface and T_o at the outlet; and (d) water discharge at the outlet recorded hourly at sites LM and LO for 1 June through 30 November 1994. Dotted lines indicate estimated value.

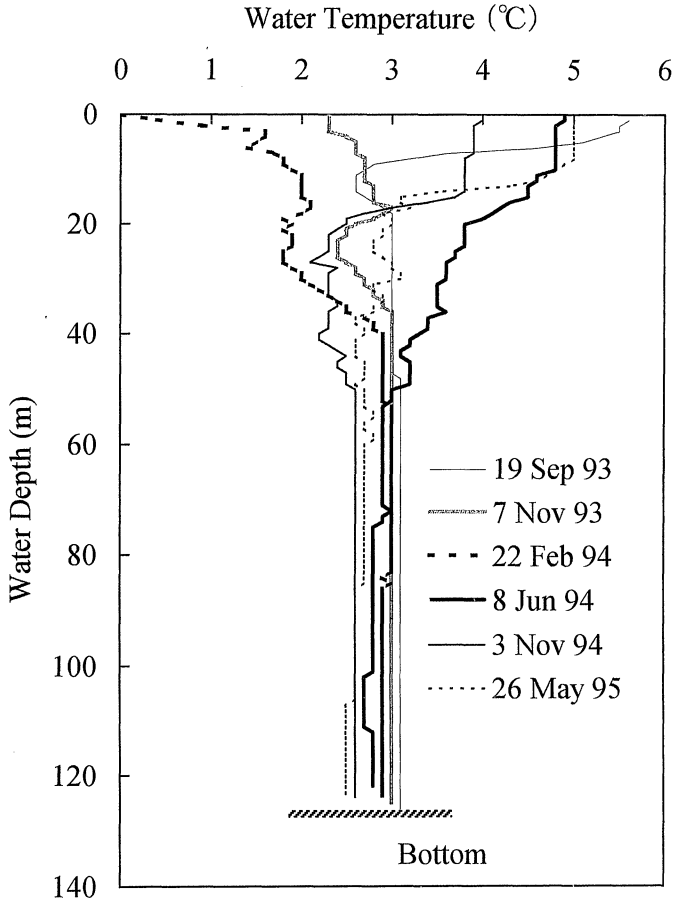

Fig. 5. Seasonal variation in vertical distributions of water temperature at site LV.

on average 48.1 cm for 14 November 1993 through 3 October 1995, thus giving an annual deepening rate of 25.5 cm.

Lake Heat Balance

Basic equation—The change in heat storage of the lake, ΔS, consists of the net heat input, Q_s, at the water surface, the heat, Q_o, released by water discharge at the outlet, the heat input, Q_i, by meltwater inflow into the lake, and the latent heat, Q_m, for ice melting on or below the bottom as in the following equation:

$$\Delta S = Q_s + Q_i - Q_m. \tag{1}$$

Calculation of each term: Heat by meltwater inflow, Q_i—The water temperature of inflowing meltwater, T_i is probably 0°C, because it is supplied from a subaqueous tunnel mouth through en-glacial tunnels (Yamada 1995). Hence $Q_i = c\rho q_i T_i = 0$, where c is the specific heat of water (=4.2 × 10^3 J °C^{-1} kg^{-1}), ρ is the water density (=1,000 kg m^{-3}), and q_i is the meltwater inflow (m^3 s^{-1}).

Change of heat storage in the lake, ΔS—The change of stored heat in the lake ΔS during the time period of t_1 to t_2 ($t_2 > t_1$) was defined as:

$$\Delta S = \frac{S_2 - S_1}{t_2 - t_1} \tag{2}$$

where S_i (i = 1, 2) is the heat storage at the time t_i. S_i is estimated by the following equation, assuming that water temperature at a certain depth is the same over the lake:

$$S_i = c\rho \int_0^{z_i} A(z)T_w(z)\, dz \tag{3}$$

where z_i, $T_w(z)$ and $A(z)$ are total depth (m) at the time t_i, water temperature (°C) at z (m) in depth at the time t_i, and area of horizontal cross section (m^2) at z (m).

Heat loss by outflow, Q_o—Heat released by the outflow at the outlet (Q_o) is simply calculated by the following equation:

$$Q_o = c\rho DT_o \tag{4}$$

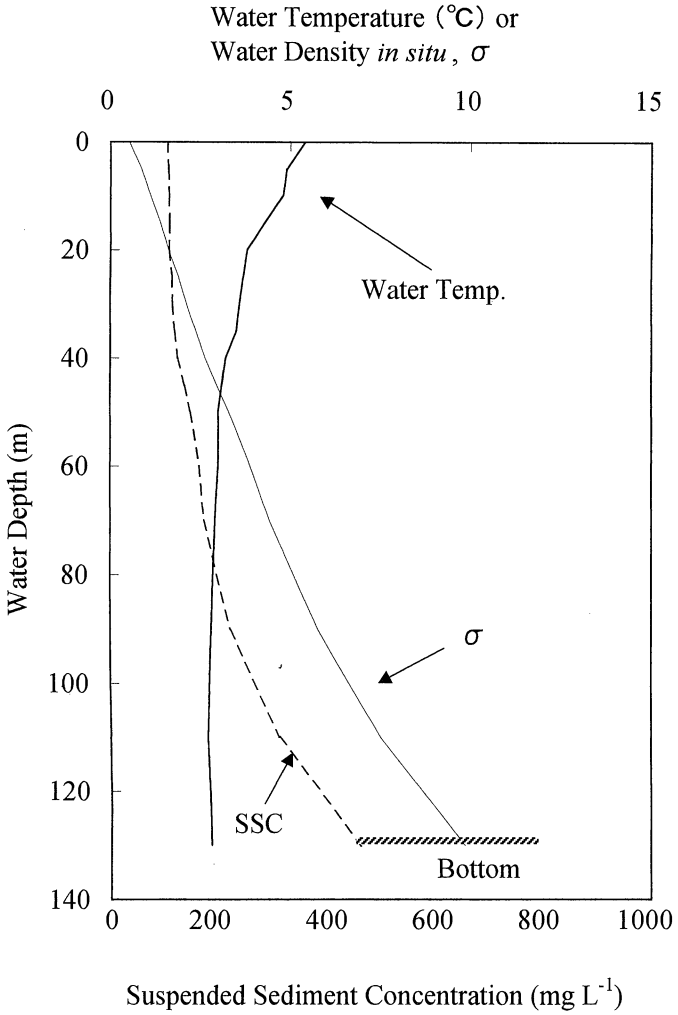

Fig. 6. Vertical distributions in water temperature, water density in situ σ and suspended sediment concentration (SSC), in June 1994.

where D is the discharge amount by outflow and T_o is water temperature of outflow.

Heat input, Q_s—During the summer, the heat Q_s coming into the lake for 1 d (t) is calculated by the following heat balance equation at the lake surface:

$$Q_s = I + R + H + lE + P \tag{5}$$

where, I, R, H, lE, and P are net shortwave radiation, net longwave radiation, sensible heat flux, latent heat flux, and heat input with precipitation, respectively. All fluxes are positive when fluxes are directed toward the lake surface.

The net shortwave radiation input to the lake surface is calculated by

$$I = (1 - \alpha)I^{\downarrow} \tag{6}$$

$I^{\downarrow}$ and α are shortwave solar radiation and albedo of the water surface, respectively. The relation of the albedo of lake surface and the solar altitude, h (degree) was obtained from observations as follows.

$$\alpha = 0.78h^{-0.45}. \tag{7}$$

Only net incoming heat at the water surface was here considered. The internal absorption in water is, therefore, not taken into account. The observed albedo is larger than that of pure water because the water containing much suspended sediment reflects solar radiation.

Net longwave radiation input, R, to the lake surface is expressed as

$$R = R^{\downarrow} - \epsilon\sigma(T_s + 273.2)^4 \tag{8}$$

where $R^{\downarrow}$, ϵ, σ, and T_s are downward longwave radiation, emissivity of the water surface (=0.96), Stefan–Boltzmann constant ($=5.67 \times 10^{-8}$ W m^{-2} K^{-4}), and water temperature of the lake surface (°C), respectively. Daily mean downward longwave radiation was evaluated as $R^{\downarrow}$ by the following equations (Kondo et al. 1991):

$$R^{\downarrow} = \sigma(T_a + 273.2)^4\left[1 - \left(1 - \frac{R^{\downarrow}_{df}}{\sigma(T_a + 273.2)^4}\right)C\right] \tag{9}$$

$$C = 0.03B^3 - 0.30B^2 + 1.25B - 0.04, \quad B \geq 0.0323$$
$$= 0, \quad B < 0.0323 \tag{10}$$

with

$$B \equiv I^{\downarrow}/I^{\downarrow}_c,$$

where T_a, $R^{\downarrow}_{df}$, and $I^{\downarrow}_c$ are air temperature (°C), global longwave radiation in the clear sky, and global solar radiation in the clear sky, respectively. The effect of clouds on $R^{\downarrow}$ is evaluated by the empirical Eq. 8 derived from the ratio, B, of observed global shortwave radiation, $I^{\downarrow}$ to $I^{\downarrow}_c$, calculated theoretically on clear days.

Sensible heat flux, H, and latent heat flux, lE, are calculated by the following bulk aerodynamic formulas presented by Kondo (1975) that are applied to the wide water surface under neutral equilibrium air conditions. The bulk heat transfer coefficient for the wide water surface is here adopted because of the large fetch of the lake (≈3 km).

$$H = c_p\rho_a C_H U(T_a - T_s) \tag{11}$$

$$lE = l\rho_a C_E U(q_a - q_s) \tag{12}$$

where c_p, ρ_a, C_H, C_E, U, and l are specific heat at constant volume, air density at 4,000 m above sea level, bulk heat transfer coefficient ($=1.80 \times 10^{-3}$), bulk latent heat transfer coefficient ($=1.84 \times 10^{-3}$) (Kondo 1975), wind velocity at 2 m in height (m s^{-1}), and latent heat for evaporation from water surface, respectively. q_a is specific humidity of air over the lake (kg kg^{-1}). q_s is specific humidity at the lake surface (kg kg^{-1}) and for convenience assumed to be the saturated specific humidity at lake surface temperature, T_s.

When the temperature of rainfall is assumed to be equal to the air temperature, the average heat flux with rainfall would be only about 0.4 W m^{-2} that corresponds to 0.4% of the net incoming heat to the lake surface. Heat flux with rainfall was thus neglected for the incoming heat at the lake water surface.

From the above calculation, the heat loss for ice melting, Q_m, can be evaluated from Eq. 1. Thus, Q_m induces the expansion of the lake.

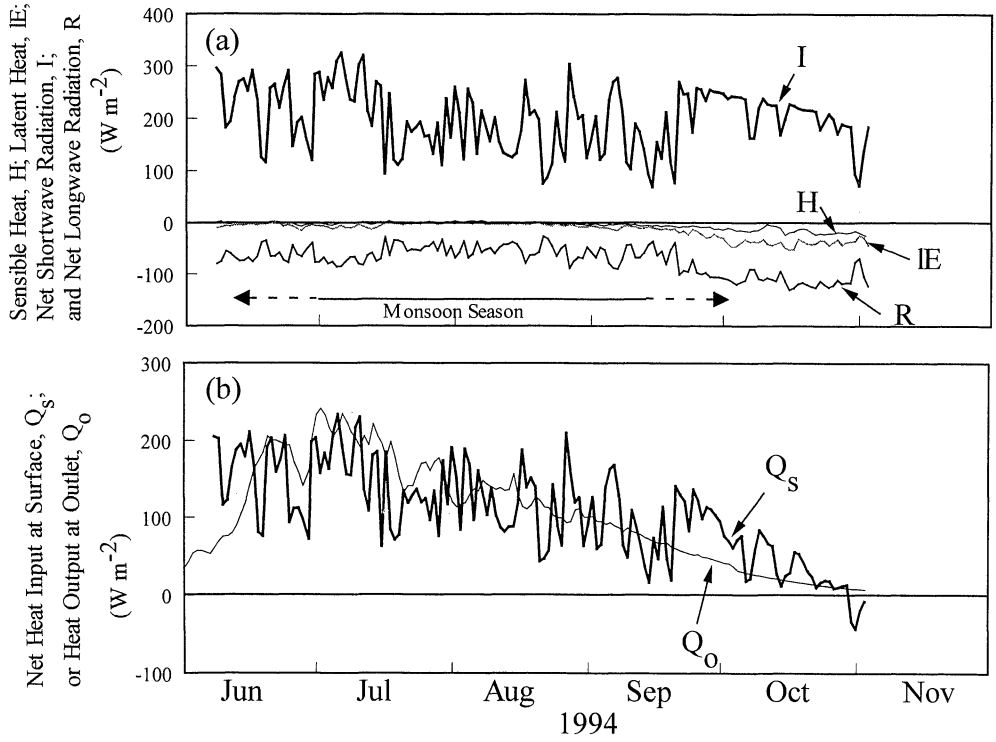

Fig. 7. Temporal variations in (a) calculated sensible heat, *H,* latent heat, *lE,* net shortwave radiation, *I,* and net longwave radiation, *R*; and (b) calculated Q_s and Q_o.

Calculated results and discussion

Each term in Eq. 1 for the summer (from 8 June 1994 to 3 November 1994; 148 d) and for the ice-covered period (from 7 November 1993 to 22 February 1994; 106 d) were evaluated, and the annual expansion rate was estimated.

Heat input to the lake surface, Q_s—The summer variations of *I, R, H,* and *lE* calculated are shown in Fig. 7a. It is evident that the heat balance at the lake surface is mainly controlled by shortwave radiation. The calculated seasonal variation of Q_s is shown in Fig. 7b. The large variation in Q_s results from the great fluctuation in net solar radiation, *I.* Q_s is consistently positive in the monsoon season from mid-June to the end of October.

No meteorological data were obtained during the ice-covered period. The observed lake-ice and snow thicknesses were 50 cm and 20 cm, respectively, on 22 February 1994. Patterson and Hamblin (1988) showed that the heat exchange between the water and ice is negligible during the ice-covered period. The incoming heat to the lake water is thus assumed to be zero.

Heat loss by outflow through outlet, Q_o—Figure 7b shows the fluctuation of the heat, Q_o. The heat loss by discharge of the surface water increased rapidly in June with increasing discharge at the outlet and then reached its peak at the beginning of July. Thereafter it decreased gradually until November. The magnitude of Q_o is of roughly the same order as Q_s in the monsoon season.

There are no data on water temperature and discharge at the outlet during the ice-covered period because of data logger trouble. The discharge amount from the outlet must be negligible during the winter season, and the water temperature from the outlet can be assumed to be 0°C because the water was released from the ice-covered lake. The heat loss from the outlet during the ice-covered period, Q_o, was thus assumed to be zero.

Change of heat storage in lake, ΔS—The changes in the heat storage, ΔS calculated during the summer season and the ice-covered period were -15 W m^{-2} (-2.6×10^{14} J) and -12 W m^{-2} (-1.5×10^{14} J), respectively. In spite of the relatively high air temperature during the monsoon season, the heat storage has a decreasing tendency. This is because the abundant glacier meltwater is supplied into the glacial lake, and the warmed water overflowed from the outlet, that is Q_o. The heat storage in the lake should have increased for a short period between April and June.

Heat loss by ice melt, Q_m—Each term of heat balance in Eq. 1 calculated is summarized in Table 1. Total heat loss by the ice melt, Q_m, was evaluated as a residual value from Eq. 1. The heat of Q_m during the open-water period was calculated to be 4.3×10^{14} J that can melt the ice volume of 14.2×10^5 m^3. The heat loss by ice melt is only 23% of the heat input to the lake surface, Q_s. Almost all of Q_s is lost by the outflow of warmed lake water at the outlet.

During the ice-covered period, the heat loss at the lake bottom corresponds to the change in storage heat of about 12 W m^{-2} (Table 1) by assuming that the heat input to the

Table 1. Heat balance terms calculated during the open-water period and ice-covered period.

	$\times 10^{14}$ J (W m^{-2})	Open water 8 Jun 1994 to 3 Nov 1994 (148 d)	Ice cover 8 Nov 1993 to 22 Feb 1994 (106 d)
Q_s	Heat input to the surface	19.0(107)	—
Q_o	Heat released from the outlet	17.3(97)	—
ΔS	Change of stored heat in the lake	−2.6(−15)	−1.5(−12)
Q_m	Heat for ice melting at the bottom of the lake	2.1(12)	1.5(12)
	Heat for fusion of calving ice	2.2(13)	—

lake surface, Q_s, and released heat with outflow, Q_o, are both zero.

Accuracy of calculation—Instrumental errors for the heat fluxes, Q_s, Q_o, and ΔS are ± 15 W m^{-2} (15%), ± 16 W m^{-2} (16%), and ± 0.3 W m^{-2} (2%), respectively, during the calculated open-water period. The horizontal difference in water temperature in the longitudinal direction of the lake is at most 0.6°C. Therefore, the error of ΔS is ± 0.6 W m^{-2} (4%). As a result, the total accuracy of the heat loss for ice melting is ± 32 W m^{-2} in the open-water period, which was larger than the heat loss (24 W m^{-2}) by the ice melt.

The surface water temperature in the lake was comparatively high near the shore. The heterogeneous surface water temperature makes the Q_s low, because it was measured at midlake where the water temperature was relatively low. Moreover, the glacial lake is surrounded by high Himalayan mountains; the reflection of longwave radiation from the exposed rockface of the mountains could lead to an underestimation of the calculated result by the empirical (Eqs. 8 and 9). This would cause the actual value of Q_s (Eq. 5) to be higher than we estimate.

The observed water temperature at the outlet was 0.5°C lower than the observed surface temperature at site LS (Fig. 3) from May to August. This relation has been used to calculate the water temperature at the outlet from September to November when there were no data. The difference, however, would show a seasonal variation. The calculated value of Q_o would depend on the condition of water mixing and surface heat balance near the outlet.

During the ice-covered period, it is enough to estimate Q_m considering only the error of heat storage. The error of ΔS is ± 0.6 W m^{-2} as mentioned above that corresponds to 5% of the heat of Q_m during the ice-covered period (12 W m^{-2}). The deepening rate from the data in the ice-covered period thus has more reliability than that in the open-water season.

Expansion rate—During the winter, all of Q_m went into melting the bottom ice because horizontal expansion (calving) must not have occurred. The net heat flux of 12 W m^{-2} was converted into a deepening rate of 3.4×10^{-3} m d^{-1}. The bottom ice of the lake was constantly melted by heat conduction in the debris–sediment–water medium below the bottom. The melt rate of the bottom ice was thus considered to be constant, assuming no bottom sedimentation, because the water temperature was almost constant throughout the year (Fig. 5). The total annual deepening rate of the lake basin was thus deduced to be 1.2 m.

The estimated present deepening rate, 1.2 m yr^{-1}, was equal to the mean deepening rate because the glacial lakes emerged (average depth at present/age of the glacial lake). Thus, the vertical expansion of the glacial lake is still continuing.

During the open-water period the lake has been expanded by the melting of the glacier terminus (terminal of the glacier) and the ice below the lake bottom (Yamada 1998). For this period Q_m should have been used in melting ice two ways. According to our observations, a cliff-shaped glacier terminus retreated by calving, and the glacier ice frequently fell into the lake only in summer when air temperature was above the melting point. Calving produces many small icebergs in front of the glacier terminus. The icebergs floating on the lake were mostly melted in the lake water. The heat for ice melting at the bottom of the lake should be 2.1×10^{14} J during the open-water period on the assumption that the deepening rate is constant all through the year. The melting heat for calving ice, therefore, can be evaluated to be 2.2×10^{14} J as the residual value of the heat Q_m (4.3×10^{14} J). It corresponds to the calving ice volume of 7.2×10^5 m^3. The annual calving ice was observed to be 300 m in width and the glacier retreat to be 100 m long. The height including the glacier ice under the lake surface can be estimated to have been 24 m from the calculated total calving ice volume, 7.2×10^5 m^3. Actually the height could be estimated to be around 20 m from the depth measurement near the glacier terminus. Although the error of the calculation was large during the summer, the result is plausible.

The calving volume during the summer observation period coincides with the annual calving rate because calving occurred only in summer. As a result, the annual expanding volume was found to be 2.4×10^6 m^3 by summing the deepening volume (1.7×10^6 m^2) and the calving ice volume (7.2×10^5 m^3) at present. It thus corresponded to 3 ± 1.5% of the whole present volume of the lake.

The sediment layer may thicken year after year by sedimentation, particularly near the end moraine where the lake began to emerge. The melt rate may thus decrease by decreasing the temperature gradient in the sediment–debris–water layer. Therefore, the annual deepening rate of 25.5 cm at site LP was much smaller than the evaluated deepening rate, probably because of the thick debris layer over the ice. Meanwhile, the deepening rate may be relatively high uplake, where the debris layer was not considered to be thick yet. The deepest point LD in Fig. 3 (131 m depth in 1994) corresponded to the glacier surface in the early 1970s, according to the satellite images (Mool 1995). Assuming that the level of the glacier surface in 1970s was equal to the water surface level in 1994 at site LD, the average deepening

rate during 24 years (1970–1994) was considered to be >5 m yr^{-1}.

More accurate deepening rates should be measured by minute depth sounding in the future. By examining the sedimentation process at the lake bottom, it may be determined whether or not the deepening rate will accelerate. Further, the hydrodynamic behavior of the lake also may be important to solving this problem (Chikita et al. 1997, 1999).

Conclusions

Heat loss for ice melting of the glacial lake was estimated from its bulk heat balance during the open-water and the ice-covered periods.

All of the heat flux into the lake is consumed as bottom ice melt during the ice-covered period. The deepening rate was deduced to be 3.2×10^{-3} m d^{-1} with an error of 5%. Because the observed temperature of bottom water contacting the ice through a debris–sediment layer was almost constant throughout the year, the deepening rate should also be constant. The annual deepening rate, therefore, was deduced to be 1.2 m. The evaluated deepening rate at present was same with the mean annual deepening rate over the lake area since 1952 (average depth of the lake [55 m in 1994]/age of the glacial lake = 1.2 m yr^{-1}). Here, the vertical expansion is still continuing.

During the open-water period, heat loss for ice melting is consumed as melting heat for calving ice and bottom ice. Assuming that the deepening rate is constant all year, our heat balance calculation allows us to estimate that 7.2×10^5 m^3 of calving ice is melted each year. The observed calving ice volume was around 6.0×10^5 m^3, which is of the same order as the calculated result. The calculated calving volume should correspond to the annual calving volume rate because calving occurred only during the summer. Consequently, the present annual volume expansion rate is 2.4×10^6 m^3 (3% of the total present volume) including the calving ice.

References

CHIKITA, K., J. JHA, AND T. YAMADA. 1999. Hydrodynamics of a supraglacial lake and its effect on the basin expansion: Tsho Rolpa, Rolwaling Nepal Himalaya. Arct. Antarct. Alpine Res. **31:** 1, 58–70.

———, T. YAMADA, A. SAKAI, AND R. P. GHIMIRE. 1997. Hydrodynamic effects on the basin expansion of Tsho Rolpa Glacier Lake in the Nepal Himalaya. Bull. Glacier Res. **15:** 59–69.

KADOTA, T. 1994. Report for the field investigation on the Tsho Rolpa glacier lake, Rolwaling Valley, February 1993–June 1994. WECS Report, N551.489 KAD.

KIRKBRIDE, M. P. 1993. The temporal significance of transitions from melting to calving termini at glaciers in the central Southern Alps of New Zealand. The Holocene **3:** 232–240.

KONDO, J. 1975. Air-sea bulk transfer coefficient in diabatic conditions. Bound. Layer Meteorol. **9:** 91–112.

———, T. NAKAMURA, AND T. YAMAZAKI. 1991. Estimation of the solar and downward Atmospheric Radiation. Tenki **38:** 41–48 (in Japanese).

LIESTØL, O. 1956. Glacier dammed lakes in Norway. Nor. Geograf. Tidsskr. **15:** 122–146.

LIGG/WECS/NEA. 1988. Report on first expedition to glaciers and glacier lakes in the Pumqu (Arun) and Poiqu (Bhote-Sun Koshi) river basins, Xizang (Tibet), China, p. 192. Science Press, Beijing, China. Sino-Nepalese Joint Investigation of Glacier Lake Outburst Flood in Himalayas in 1987, Lanzhou Institute of Glaciology and Geocryology, Academia Sinica, and Water and Energy Commission Secretariat of Nepal, Science Press, Beijing, China.

LLIBOUTRY, L. 1977. Glaciological problems set by the control of dangerous lakes in Cordillera Blanca, Peru. II. Movement of a covered glacier embedded within a rock glacier. J. Glaciol. **79:** 235–273.

———, B. MORALES, A. PAUTRE, AND B. SCHNEIDER. 1977*a*. Glaciological problems set by the control of dangerous lakes in Cordillera Blanca, Peru. I. Historical failures of morainic dams, their causes and prevention. J. Glaciol. **79:** 239–254.

———, ———, AND B. SCHNEIDER. 1977*b*. Glaciological problems set by the control of dangerous lakes in Cordillera Blanca, Peru. III. Study of moraines and mass balances at Safuna. J. Glaciol. **79:** 275–290.

MOOL, K. P. 1995. Glacier lake outburst floods in Nepal. J. Nepal Geolog. Soc. Kathmandu **11:** 273–280.

MORIBAYASHI, S. 1974. On the characteristics of Nepal Himalayan glaciers and their recent variations. Seppyo **36:** 11–21.

PATTERSON, J. C., AND P. F. HAMBLIN. 1988. Thermal simulation of a lake with ice cover. Limnol. Oceanogr. **33:** 323–338.

POST, A., AND L. R. MAYO. 1971. Glacier dammed lakes and outburst floods in Alaska. Hydrological Investigations Atlas HA-455, U.S. Geological Survey, Department of the Interior, Washington, D.C., 10 p. + 3 maps.

SAKAI, A., K. FUJITA, T. AOKI, K. ASAHI, AND M. NAKAWO. 1997. Water discharge from the Lirung Glacier in Langtang Valley, Nepal Himalayas, 1996. Bull. Glacier Res. **15:** 79–83.

SCHNEIDER, E. 1981. Topographic map of Rolwaling Himal, Nepal-Kartenwerk der Arbeitsgemeinschaft für vergleichende Hochgebirgsforschung Nr.4, Research scheme Nepal Himalaya.

THORARINSSON, S. 1939. The ice dammed lakes of Iceland with particular reference to their values as indicators of glacier oscillations. Geograf. Ann. Årg. **21:** 216–242.

———. 1957. The jökulhlaup from the Katla area in 1955 compared with other jökulhlaups in Iceland. Jökull. Ár. **7:** 21–25.

WECS. 1994. Energy sector synopsis report; Nepal 1992/93. WECS Report, No. 4/4/270494/1/1 Seq. No. 451.

YAMADA, T. 1993. Glacier lakes and their outburst floods in the Nepal Himalaya, p. 37 WECS/JICA.

———. 1995. Data report on meteorological and hydrological data at Tsho Rolpa Glacier Lake, Rolwaling Himal—from June 1993 to May 1995. WECS Report N551.498 DAT.

———. 1996. Report of the investigations of Tsho Rolpa Glacier Lake, Rolwaling Valley, p. 35 WECS/JICA.

———. 1998. Glacier lake and its outburst flood in the Nepal Himalaya, Monograph No. 1, March 1998 Data Center for Glacier Research, Japanese Society of Snow and Ice.

Received:13 August 1998
Accepted: 11 May 2000
Amended: 31 May 2000